Enhancing Parallelism of Tile QR Factorization for Multicore Architectures

Bilel Hadri, Hatem Ltaief, Emmanuel Agullo, and Jack Dongarra

Abstract

To exploit the potential of multicore architectures, recent dense linear algebra libraries have used tile algorithms, which consist of scheduling a Directed Acyclic Graph (DAG) of fine granularity tasks where nodes represent tasks, either panel factorization or update of a block-column, and edges represent dependencies among them. Although past approaches already achieve high performance on moderate and large square matrices, their way of processing a panel in sequence leads to limited performance when factorizing tall and skinny matrices or small square matrices. We present a new, fully asynchronous method for computing a QR factorization on shared-memory multicore architectures that overcomes this bottleneck. Our contribution is to adapt an existing algorithm that performs a panel factorization in parallel (named Communication-Avoiding QR and initially designed for distributed-memory machines) to the context of tile algorithms using asynchronous computations. An experimental study shows significant improvement (up to almost 10 times faster) compared to state-of-the-art approaches. We aim to eventually incorporate this work into the Parallel Linear Algebra for Scalable Multi-core Architectures (PLASMA) library.

I. Introduction and Motivations

QR factorization is one of the major one-sided factorizations in dense linear algebra. Based on orthogonal transformations, this method is well known to be numerically stable and is a first step toward the resolution of least square systems [12]. We have recently developed a parallel tile QR factorization [7] as part of the Parallel Linear Algebra Software for Multi-core Architectures (PLASMA) project [3].

PLASMA Tile QR factorization has been benchmarked on two architectures [4], a quad-socket quad-core machine based on an Intel Xeon processor and a SMP node composed of 16 dual-core Power6 processors. Table I and II report the parallel efficiency (the quotient of the division of the time spent in serial by the product of the time spent in parallel and the number of cores used) achieved with different square matrix sizes on each architecture. PLASMA Tile QR factorization scales fairly well for large square matrices and up to the maximum number of cores available on those shared-memory machines, 16 and 32 cores on Intel and Power6, respectively. However, for small matrices, the parallel efficiency significantly decreases when the number of cores increases. For example, for matrix sizes lower than 1000, the efficiency is roughly at most 50% on Intel and Power6 with 16 cores. And this declines on Power6 with only a 6% parallel efficiency achieved on 32 cores for a matrix of size 500. The cores run out of work and stay idle most of the time. The significant decrease of efficiency is also explained by the sequential nature of the panel factorization which limits the opportunities for parallelism and generates load imbalance especially when

Bilel Hadri, Hatem Ltaief, Emmanuel Agullo and Jack Dongarra are with the Department Electrical Engineering and Computer Science, University of Tennessee, Knoxville.
E-mail: {hadri, ltaief, eagullo, dongarra}@eecs.utk.edu
Jack Dongarra is also with the Computer Science and Mathematics Division, Oak Ridge National Laboratory, Oak Ridge, Tennessee, and with the School of Mathematics School of Computer Science, University of Manchester
Research reported here was partially supported by the NSF and Microsoft Research.

TABLE I
PARALLEL EFFICIENCY ON INTEL

	Number of cores			
Matrix order	2	4	8	16
500	69%	55%	**39%**	**24%**
1000	88%	73%	60%	**45%**
2000	97%	91%	81%	69%
4000	98%	97%	94%	84%
8000	97%	97%	96%	89%

TABLE II
PARALLEL EFFICIENCY ON POWER6

	Number of cores			
Matrix order	4	8	16	32
500	**43%**	**25%**	**12%**	**6%**
1000	67%	**46%**	**24%**	**12%**
2000	80%	65%	**46%**	**25%**
4000	90%	79%	71%	51%
8000	95%	88%	85%	75%

processing small or tall and skinny (TS) matrices (of size $m-$by$-n$ with $m >> n$) where a large proportion of the elapsed time is spent in those sequential panel factorizations.

The purpose of this paper is to present a fully asynchronous method to compute a QR factorization of TS matrices on shared-memory multicore architectures. This new technique finds its root in combining the core concepts from the Tile QR factorization implemented in the PLASMA library and the Communication-Avoiding QR (CAQR) [9] algorithm introduced by Demmel et al. Initially designed for distributed-memory machines, CAQR factors general rectangular distributed matrices with a parallel panel factorization. Even if the present paper discusses algorithms for shared-memory machines where communications are not explicit, multicore platforms often symbolize, at a smaller scale, a distributed-memory environment with a memory and/or cache hierarchy to benefit from memory locality in computer programs. Hence the relevance of using algorithms that limit the amount of communication in our context too.

This present journal version is an extension of a conference proceeding paper [14]. Here are the main differences compared to that paper. We present here a new variant (Section III-B) of the main algorithm. We also discuss in more detail the amount of parallelism provided by our algorithms. To do so, we first compare their corresponding Directed Acyclic Graphs (DAG) (Section IV) to the ones of tile algorithms, i.e., PLASMA. We then study their impact on actual parallel execution traces (Section V-C).

The paper is organized as follows. Section II presents the background work. Section III describes two new approaches that combine algorithmic ideas from tile algorithms and the Communication-Avoiding algorithms. Section IV shows that our algorithms lead to DAGs exhibiting more parallelism than tile algorithms such as PLASMA. Section V explains how the tasks from the resulting DAGs are scheduled in parallel. In Section VI, an experimental study shows the behavior of our algorithm on multicore architectures and compares it against existing numerical libraries. Finally, in Section VII, we conclude and present future work directions.

II. Background

TS matrices are present in a variety of applications in linear algebra, e.g., in solving linear systems with multiple right-hand sides using block iterative methods by computing the QR factorization of a TS matrix [10], [18]. But above all, TS matrices show up at each panel factorization step while performing one-sided factorization algorithms (QR, LU and Cholesky). The implementation of efficient algorithms handling such matrix shapes is paramount. In this section, we describe different algorithms for the QR factorization of TS matrices implemented in the state-of-the-art numerical linear algebra libraries.

A. LAPACK/ScaLAPACK QR factorization

Generally, a QR factorization of an $m \times n$ real matrix A is the decomposition of A as $A = QR$, where Q is an $m \times m$ real orthogonal matrix and R is an $m \times n$ real upper triangular matrix. QR factorization uses a series of elementary Householder matrices of the general form $H = I - \tau v v^T$ where v is a column reflector and τ is a scaling factor.

Regarding the block or block-partitioned algorithms as performed in LAPACK [5] or ScaLAPACK [6] respectively, nb elementary Householder matrices are accumulated within each panel and the product is represented as $H_1 H_2 ... H_{nb} = I - VTV^T$. Here V is a $n \times nb$ matrix in which columns are the vectors v, T is a $nb \times nb$ upper triangular matrix and nb is the block size.

Although the panel factorization can be identified as a sequential execution that represents a small fraction of the total number of FLOPS performed ($\theta(n^2)$) FLOPS for a total of $\theta(n^3)$) FLOPS), the scalability of of block factorizations is limited on a multicore system. The parallelism is only exploited at the level of the BLAS routines for LAPACK or PBLAS routines for ScaLAPACK. This methodology complies a fork-join model since the execution flow of a block factorization represents a sequence of sequential operations (panel factorizations) interleaved with parallel ones (updates of the trailing submatrices).

B. Tile QR factorization (PLASMA-like factorization)

PLASMA Tile QR factorization [7], [8] evolves from the block algorithms that provides high performance implementations for multicore system architectures. The algorithm is based on annihilating matrix elements by square tiles instead of rectangular panels as in LAPACK. PLASMA Tile QR algorithm relies on four primary operations developed by four computational kernels:

- **CORE_DGEQRT**: this routine performs the QR factorization of a diagonal tile A_{kk} of size $nb \times nb$ of the input matrix. It produces an upper triangular matrix R_{kk} and a unit lower triangular matrix V_{kk} containing the Householder reflectors. An upper triangular matrix T_{kk} is also computed as defined by the WY technique [20] for accumulating the transformations. R_{kk} and V_{kk} are written on the memory area used for A_{kk} while an extra work space is needed to store the structure T_{kk}. The upper triangular matrix R_{kk}, called *reference tile*, is eventually used to annihilate the subsequent tiles located below, on the same panel.
- **CORE_DTSQRT**: this routine performs the QR factorization of a matrix built by coupling the reference tile R_{kk} that is produced by CORE_DGEQRT with a tile below the diagonal A_{ik}. It produces an updated R_{kk} factor, a matrix V_{ik} containing the Householder reflectors and a matrix T_{ik} resulting from accumulating the reflectors V_{ik}.
- **CORE_DORMQR**: this routine applies the transformations computed by CORE_DGEQRT (V_{kk}, T_{kk}) to a tile A_{kj} located on the right side of the diagonal tile.
- **CORE_DTSSSMQR**: this routine applies the reflectors V_{ik} and the matrix T_{ik} computed by CORE_DTSQRT to two tiles A_{kj} and A_{ij}.

Since the Tile QR factorization is also based on Householder reflectors that are orthogonal transformations, this factorization is stable. Figure 1 shows the first panel reduction applied on a 3-by-3 tile matrix. The triangular shapes located on the left side of the matrices correspond to the extra data structure needed to store the different T_{ij} triangular matrices. The striped tiles represent the input dependencies for the trailing submatrix updates. The algorithm for general matrices, with MT tiles in row and NT tiles in column, is formulated in Algorithm 1. As of today, PLASMA implements Algorithm 1 through a given framework based on a static scheduling and discussed later in Section V-A. In the rest of the paper, we will use the term *PLASMA-like factorization* to refer to any factorization based on Algorithm 1, without regard to the framework implementing it nor the scheduling mechanism used.

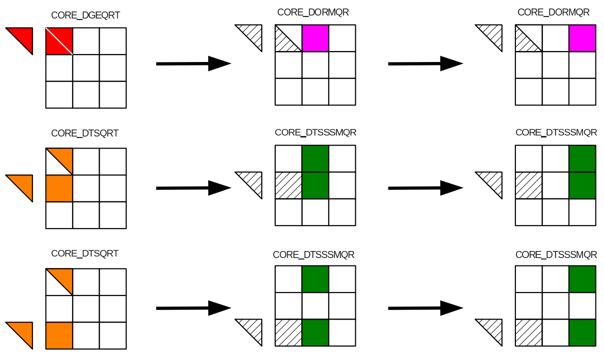

Fig. 1. Reduction of the first tile column.

Algorithm 1 Tile QR factorization (PLASMA-like factorization)

```
for $k = 1$ to $min(MT, NT)$ do
    $R_{k,k}, V_{k,k}, T_{k,k} \leftarrow$ CORE_DGEQRT($A_{k,k}$)
    for $j = k + 1$ to $NT$ do
        $A_{k,j} \leftarrow$ CORE_DORMQR($V_{k,k}, T_{k,k}, A_{k,j}$)
    end for
    for $i = k + 1$ to $MT$ do
        $R_{k,k}, V_{i,k}, T_{i,k} \leftarrow$ CORE_DTSQRT($R_{k,k}, A_{i,k}$)
        for $j = k + 1$ to $NT$ do
            $A_{k,j}, A_{i,j} \leftarrow$ CORE_DTSSSMQR($V_{i,k}, T_{i,k}, A_{k,j}, A_{i,j}$)
        end for
    end for
end for
```

Although PLASMA achieves high performance on most types of matrices by implementing Algorithm 1 [4], each panel factorization is still performed in sequence, which limits the performance when processing small or TS matrices (see results reported in Section I).

C. Parallel Panel Factorizations

The notion of splitting a column into separate pieces and performing reductions to the separate pieces in a recursive manner can be attributed to Morven Gentleman's early work on sparse matrices around the mid 70s [11]. The idea of parallelizing the factorization of a panel was first developed by Pothen and Raghavan, to the best of our knowledge, in the late 1980s [19]. The authors implemented distributed orthogonal factorizations using Householder and Givens algorithms. Each panel is actually composed of one single column in their case. Their idea is to split the column into P pieces or subcolumns (if P is the number of processors) and to perform local factorizations from which they merge the resulting triangular factors, as explained in Algorithm 2.
Demmel et al. [9] extended this work and proposed a class of QR algorithms that can perform the factorization of a panel (block-columns) in parallel, named Communication-Avoiding QR (CAQR). Compared to Algorithm 2, steps 1 and 2 are performed on panels of several columns thanks to a new kernel, called TSQR (since a panel is actually a TS matrix). CAQR successively performs a TSQR factorization (local factorizations and merging procedures) over the panels of the matrix, applying the subsequent updates on the trailing submatrix after each panel factorization, as illustrated in Figure 3. The panels are themselves split in

Algorithm 2 Pothen and Raghavan's algorithm.

Successively apply the three following steps over each column of the matrix:

1) **Local factorization.** Split the current column into P pieces (if P is the number of processors) and let each processor independently zeroes its subcolumn leading to a single non zero element per subcolumn.
2) **Merge.** Annihilate those nonzeros thanks to what they call a *recursive elimination phase* and that we name *merging step* for consistency with upcoming algorithms. This merging step is itself composed of $\log_2(P)$ stages. At each stage, processors cooperate pairwise to complete the transformation. After its element has been zeroed, a processor takes no further part in the merging step and remains idle until the end of that step. The processor whose element is updated continues with the next stage. After $\log_2(P)$ such stages, the only remaining nonzero is the diagonal element. All in all, the merging step can be represented as a binary tree where each node corresponds to a pairwise transformation.
3) **Update.** Update the trailing submatrix.

block-rows, called *domains*, that are factorized independently (step 1) and then merged (step 2) using a binary tree strategy similar to the one of Pothen et al. Figure 2 illustrates TSQR's merging procedure(step 2). Initially, at stage $k = 0$, a QR factorization is performed on each domain. Then, at each stage $k > 0$ of the binary tree, the R factors are merged into pairs $R_{i,k}$ and $R_{i+1,k}$ and each pair formed that way is factorized. This is repeated until the final R ($R_{0,2}$ in Figure 2) is obtained. If the matrix is initially split into P domains, $\log_2(P)$ (the

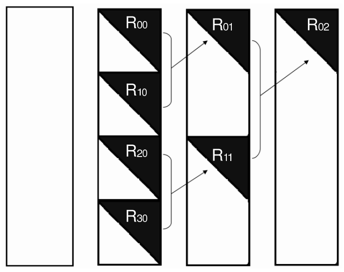

Fig. 2. TSQR factorization on four domains. The intermediate and final R factors are represented in black.

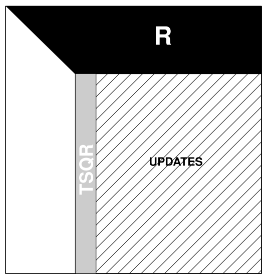

Fig. 3. CAQR: the panel (gray area) is factorized using TSQR. The trailing matrix (dashed area) is updated.

depth of the binary tree) stages are performed during the merge procedure. Demmel proved that TSQR and CAQR algorithms induce a minimum amount of communication (under certain conditions, see Section 17 of [9] for more details) and are numerically as stable as the Householder QR factorization. Both Pothen and Raghavan's and Demmel et al.'s approaches have a synchronization point between each panel factorization (TSQR kernel in Demmel et al.'s case) and the subsequent update of the trailing submatrix, leading to a suboptimal usage of the parallel processing power.

Synchronization 1: Processors (or cores) that are no longer active in the merging step still have to wait until the end of that merging step before initiating the computation related to the next panel.

In the next section, we present an asynchronous algorithm that overcomes these bottlenecks and enables look-ahead in the scheduling.

III. Tile CAQR

In this section, we present two new algorithms that extends the Tile QR factorization (as implemented in PLASMA and described in Section II-B) by performing the factorization of a panel in parallel (based on the CAQR approach described in Section II-C). Furthermore, we adapt previous parallel panel factorization approaches [9], [19] in order to enable a fully asynchronous factorization, which is critical to achieve high performance on multicore architectures. The names of our algorithms below come from the degree of parallelism of their panel factorization

A. Semi-Parallel Tile CAQR (SP-CAQR)

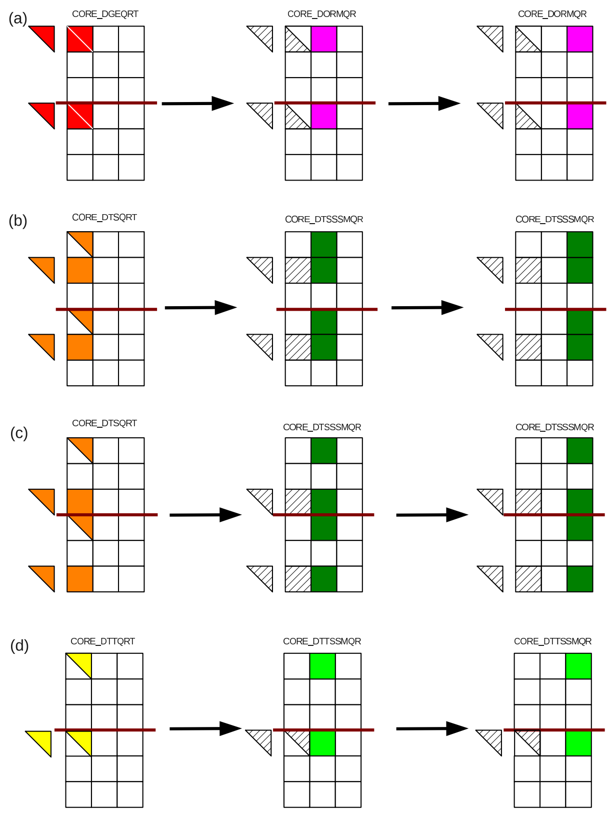

Fig. 4. Unrolling the operations related to the first panel in SP-CAQR. Two domains are used, separated by the red line. First step, the factorization of the first tile in each domain and the corresponding updates are shown in (a). Second step, the factorization of the second and third tiles in each domain using the reference tile and the corresponding updates are presented in (b) and (c) respectively. Unrolling the merging procedure related to the first panel factorization in SP-CAQR is shown in (d).

As CAQR, SP-CAQR decomposes the matrix in domains (block-rows). Within a domain, a PLASMA-like factorization (tile algorithm given in Algorithm 1) is performed. The domains are almost processed in an embarrassingly parallel fashion, from one to another.

First, a QR factorization is independently performed in each domain on the current panel (of a tile width), similarly to step 1 of Algorithm 2. Second, the corresponding updates are applied to the trailing submatrix in each domain, similarly to step 3 of Algorithm 2. For example, Figure 4 (a,b,c) illustrates the factorization of the first panel and the corresponding updates for two domains of 3-by-3 tiles (MT=6 and NT=3). The update procedure is triggered while the panel is still being factorized. Indeed, compared to CAQR Demmel et al.'s approach, our algorithm has the flexibility to interleave steps 1 and 3 of the initial Algorithm 2.

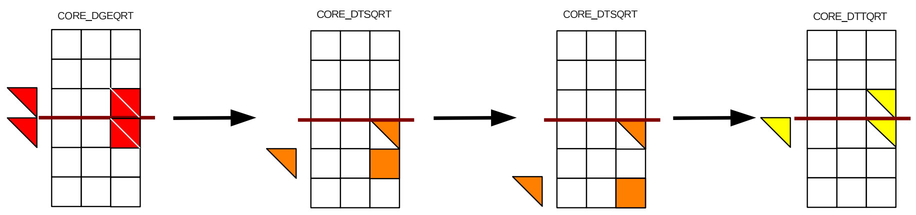

Fig. 5. Factorization of the last panel and the merging step in SP-CAQR.

Third and last, the final local R factors from each domain are merged based on the TSQR algorithm described in Section II-C and the corresponding block-row is again updated. This is the only time where a particular domain needs another one to advance in the computation. The merging procedure can also be performed as the factorization and update processes go (steps 1 and 2). Moreover, cores that no longer participate in the merging procedure can proceed *right away* with the computation of the next panel. Synchronization 1 is now released in our SP-CAQR approach which can potentially enable look-ahead in the scheduling. Figure 4(d) illustrates the merging procedure related to the first panel factorization. The factorization of the second panel can be initiated while the merging procedure of the first panel has not yet terminated.

Two new kernels are used in this step for reducing a triangular tile on top of another triangular tile as well as applying the related updates. From that point on, we consider the matrices locally to their domain and we note them with three subscripts. For instance $A_{p,i,j}$ is the tile (or block-matrix) at (local) block-row i and (local) block-column j in domain p. And we want to merge two domains, let us say $p1$ and $p2$. With these notations, here are the two new kernels:

- **CORE_DTTQRT**: this routine performs the QR factorization of a matrix built by coupling the factor $R_{p1,k,k}$ from the domain $p1$ with the factor $R_{p2,1,k}$ from the domain $p2$. It produces an updated factor $R_{p1,k,k}$, an upper triangular matrix $V_{p2,1,k}$ containing the Householder reflectors and an upper triangular matrix $T^r_{p2,1,k}$ resulting from accumulating the reflectors $V_{p2,1,k}$. The reflectors are stored in the upper annihilated part of the matrix. Another extra storage is needed for storing $T^r_{p2,1,k}$.
- **CORE_DTTSSMQR**: this routine applies the reflectors $V_{p2,1,k}$ and the matrix $T^r_{p2,1,k}$ computed by CORE_DTTQRT to two tiles $A_{p1,k,j}$ and $A_{p2,1,j}$.

Finally, Figure 5 unrolls the third and last panel factorization. A QR factorization is performed on the last tile of the first domain as well as on the entire panel of the second domain. The local R factors are then merged to produce the final R factor.

We call the overall algorithm Semi-Parallel because the degree of parallelism of the panel factorization depends on the number of domains used. For instance, on a 32 core machine, let us assume that a matrix split in 8 domains. Even if each domain is itself performed in parallel (with a PLASMA-like factorization), then 8 cores (maximum) may simultaneously factorize a given panel (one per domain). The main difference against Algorithm 1 is that Algorithm 1 is optimized for cache reuse [4] (data is loaded into cache a limited number of times) whereas our new algorithm (SP-CAQR) provides more parallelism by processing a panel in parallel. The expected gain will thus be a trade off between increased degree of parallelism and efficient cache usage.

Assuming that a matrix A is composed of MT tiles in row and NT tiles in column, SP-CAQR corresponds to Algorithm 3. The PLASMA-like factorization occurring within

Algorithm 3 Semi-Parallel Tile CAQR (SP-CAQR)

```
$nextMT = MT_{loc}$; $proot = 0$
for $k = 1$ to $min(MT, NT)$ do
    if $k > nextMT$ then
        $proot++$; $nextMT+= MT_{loc}$;
    end if
    /* PLASMA-like factorization in each domain */
    for $p = proot$ to $P-1$ do
        $ibeg = 0$
        if $p == proot$ then
            $ibeg = k - proot \times MT_{loc}$
        end if
        $R_{p,ibeg,k}, V_{p,ibeg,k}, T_{p,ibeg,k} \leftarrow$ CORE_DGEQRT($A_{p,ibeg,k}$)
        for $j = k+1$ to $NT$ do
            $A_{p,ibeg,j} \leftarrow$ CORE_DORMQR($V_{p,ibeg,k}, T_{p,ibeg,k}, A_{p,ibeg,j}$)
        end for
        for $i = ibeg+1$ to $MT_{loc}$ do
            $R_{p,ibeg,k}, V_{p,i,k}, T_{p,i,k} \leftarrow$ CORE_DTSQRT($R_{p,ibeg,k}, A_{p,i,k}$)
            for $j = k+1$ to $NT$ do
                $A_{p,ibeg,j}, A_{p,i,j} \leftarrow$ CORE_DTSSSMQR($V_{p,i,k}, T_{p,i,k}, A_{p,ibeg,j}, A_{p,i,j}$)
            end for
        end for
    end for
    /* Merge */
    for $m = 1$ to $ceil(\log_2(P - proot))$ do
        $p1 = proot$ ; $p2 = p1 + 2^{m-1}$
        while $p2 < P$ do
            $i1 = 0$ ; $i2 = 0$
            if p1==proot then
                $i1 = k - proot \times MT_{loc}$
            end if
            $R_{p1,i1,k}, V_{p2,i2,k}, T^r_{p2,i2,k} \leftarrow$ CORE_DTTQRT($R_{p1,i1,k}, R_{p2,i2,k}$)
            for $j = k+1$ to $NT$ do
                $A_{p1,i1,j}, A_{p2,i2,j} \leftarrow$ CORE_DTTSSMQR($V_{p2,i2,k}, T^r_{p2,i2,k}, A_{p1,i1,j}, A_{p2,i2,j}$)
            end for
            $p1+= 2^m$; $p2+= 2^m$
        end while
    end for
end for
```

each domain p is interleaved with the merge operations for each panel k. We note MT_{loc} the number of tiles per column within a domain (assumed constant) and $proot$ the index of the domain containing the diagonal block of the current panel k. The PLASMA-like factorization occurring in a domain is similar to Algorithm 1 except that the reference tile in domain p is not always the diagonal block of the domain (as already noticed in Figure 5). Indeed, if the diagonal block of the current panel k is part of domain $proot$ ($p == proot$), then the reference tile is the diagonal one ($ibeg = k - proot \times MT_{loc}$). Otherwise (i.e., $p \neq proot$), the tile of the first block-row of the panel is systematically used as a reference ($ibeg = 0$) to annihilate the subsequent tiles located below, within the same domain. The index of the block-row merged is then affected accordingly ($i1 = k - proot \times MT_{loc}$ when $p1 == proot$).

B. Fully-Parallel Tile CAQR (FP-CAQR)

One may proceed further in the parallelization procedure by aggressively and independently factorizing each tile located on the local panel of each domain. The idea is to process the remaining part of a panel within a domain in parallel too, with a local merging procedure. Figure 6 describes this Fully-Parallel QR factorization (FP-CAQR), and the corresponding algorithm is given in Algorithm 4.

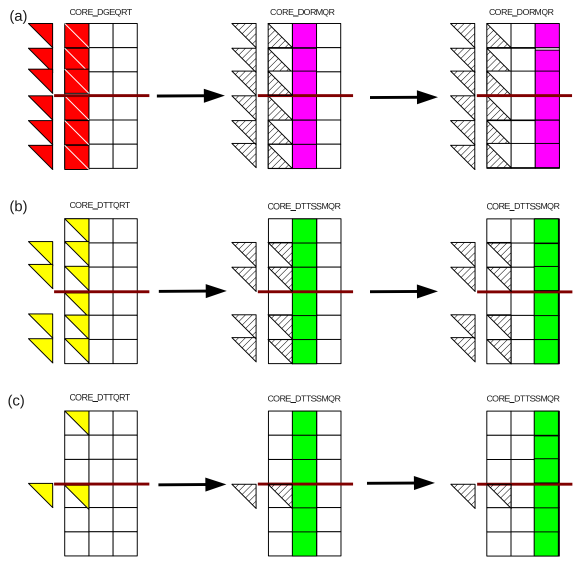

Fig. 6. Unrolling the operations related to the first panel in FP-CAQR. Two domains are used, separated by the red line. The tree steps are illustrated, the factorization(a), the local merge (b) and the global merge(c).

Actually, FP-CAQR does not depend on the number of domains used, provided that the number of tiles per column is a power of two (otherwise the pairs used for the merge operations might not match, from one instance to another). Furthermore, a given instance of FP-CAQR can be obtained with an instance of SP-CAQR by choosing the instance of SP-CAQR with a number of domains P equal to the number of tiles per row MT. This approach has been mainly mentioned for pedagogic and completeness purposes. Therefore, we will focus on SP-CAQR in the remainder of the paper. In the following section, we will discuss frameworks for exploiting this exposed parallelism.

IV. Graph Driven Asynchronous Execution

Tile algorithms in general provide fine granularity parallelism, and standard linear algebra algorithms can then be represented as a DAG to help understand the execution flow [8]. The DAGs of Algorithms 1, 3 and 4 are shown in Figures 7(a), 7(b) and 7(c) respectively. The nodes represent tasks, either panel factorization or update of a block-column, and edges represent dependencies among them.

From Figure 7, it is obvious that SP-8 and FP-CAQR considerably enhance the parallelism compared to the PLASMA-like Tile QR factorization. For example, for MT=16 and NT=2, three kernels at most can run concurrently for the PLASMA-like Tile QR factorization while a maximum of 16 and 20 kernels can run at the same time for SP-8 and FP-CAQR, respectively. Figure 8 shows a larger DAG representation of Tile QR factorization. Basically, the wider the DAG, the better opportunity to gain parallelism.

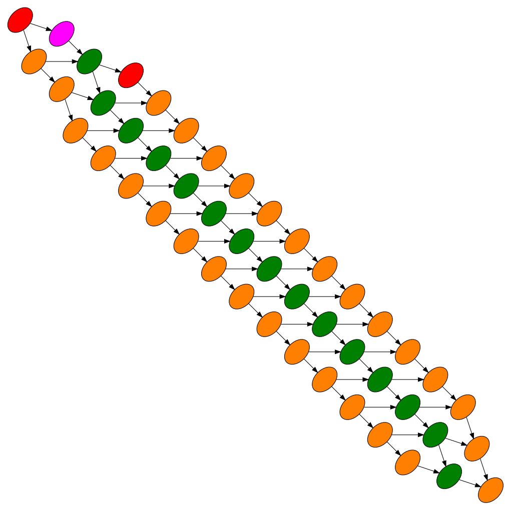
(a) One domain: SP-1 (or PLASMA-like Tile QR factorization).

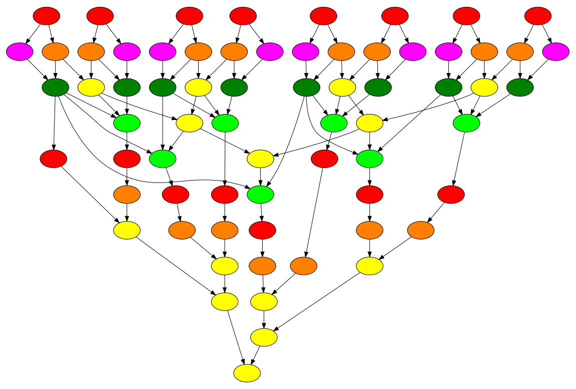
(b) Eight domains: SP-8.

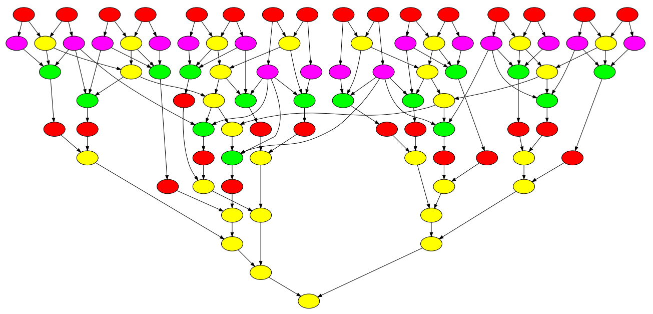
(c) Sixteen domains: SP-16 (or FP-CAQR).

Fig. 7. DAG representations of Tile QR factorization with MT=16 and NT=2 depending on the number of domains.

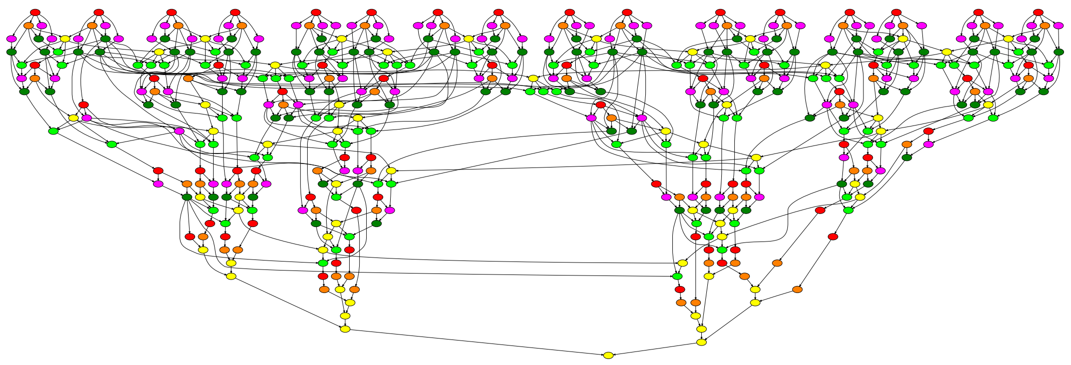
Fig. 8. DAG representations of Tile QR factorization with MT=32 and NT=4 with sixteeen domains: SP-16.

Algorithm 4 Fully-Parallel Tile CAQR (FP-CAQR)

```
$nextMT = MT_{loc}$
$proot = 0$
**for** $k = 1$ to $min(MT, NT)$ **do**
    **if** $k > nextMT$ **then**
        $proot + +$
        $nextMT+ = MT_{loc}$
    **end if**
    /* PLASMA-like factorization in each domain */
    **for** $p = proot$ to $P - 1$ **do**
        $ibeg = 0$
        **if** $p == proot$ **then**
            $ibeg = k - proot \times MT_{loc}$
        **end if**
        **for** $i = ibeg$ to $MT_{loc} - 1$ **do**
            $R_{p,i,k}, V_{p,i,k}, T_{p,i,k} \leftarrow$ CORE_DGEQRT($A_{p,i,k}$)
            **for** $j = k + 1$ to $NT$ **do**
                $A_{p,i,j} \leftarrow$ CORE_DORMQR($V_{p,i,k}, T_{p,i,k}, A_{p,i,j}$)
            **end for**
        **end for**
        /* Local Merge */
        **for** $m = 1$ to $ceil(\log_2(MT_{loc} - ibeg)$ **do**
            $i1 = ibeg; i2 = i1 + 2^{k-1}$
            **while** $i2 < MT_{loc}$ **do**
                $R_{p,i1,k}, V_{p,i2,k}, T^r_{p,i2,k} \leftarrow$ CORE_DTTQRT($R_{p,i1,k}, R_{p,i2,k}$)
                **for** $j = k + 1$ to $NT$ **do**
                    $A_{p,i1,j}, A_{p,i2,j} \leftarrow$ CORE_DTTSSMQR($V_{p,i2,k}, T^r_{p,i2,k}, A_{p,i1,j}, A_{p,i2,j}$)
                **end for**
                $i1+ = 2^k$; $i2+ = 2^k$
            **end while**
        **end for**
    **end for**
    /* Global Merge */
    **for** $m = 1$ to $ceil(\log_2(P - proot))$ **do**
        $p1 = proot$ ; $p2 = p1 + 2^{m-1}$
        **while** $p2 < P$ **do**
            $i1 = 0$ ; $i2 = 0$
            **if** p1==proot **then**
                $i1 = k - proot \times MT_{loc}$
            **end if**
            $R_{p1,i1,k}, V_{p2,i2,k}, T^r_{p2,i2,k} \leftarrow$ CORE_DTTQRT($R_{p1,i1,k}, R_{p2,i2,k}$)
            **for** $j = k + 1$ to $NT$ **do**
                $A_{p1,i1,j}, A_{p2,i2,j} \leftarrow$ CORE_DTTSSMQR($V_{p2,i2,k}, T^r_{p2,i2,k}, A_{p1,i1,j}, A_{p2,i2,j}$)
            **end for**
            $p1+ = 2^m$; $p2+ = 2^m$
        **end while**
    **end for**
**end for**
```

Once the DAGs are established, the tasks can be scheduled asynchronously and independently as long as the dependencies are not violated. A critical path can be identified in the DAG as the path that connects all the nodes that have the higher number of outgoing edges. Based on this observation, a scheduling policy can be used, where higher priority is assigned to those nodes that lie on the critical path. Clearly, in the case of the PLASMA-like Tile QR factorization and SP-CAQR, the nodes associated to the DGEQRT subroutine (red nodes) as well as those involved in the merging procedure, i.e., the DTTQRT subroutine (yellow nodes), have the highest priority. Other priority levels can be defined for the remaining kernels. The DAG scheduling results in an out of order execution where idle time is almost completely eliminated, since only very loose synchronization is required between the threads (see large traces in Section V-C).

Noteworthy to mention here is the natural suitability of such algorithms for a distributed computing environment. Each domain (or a group of domains) could be allocated to a particular processing node. The main computation would be done within the nodes. Communication between processing nodes would only be limited at the level of the merging procedure, so the name of Communication-Avoiding algorithms.

In the following section, we will discuss frameworks for exploiting this exposed parallelism.

V. Parallel Scheduling

This section explains how the resulting DAGs from the PLASMA-like QR factorization and SP-CAQR can be efficiently scheduled on a multicore machine. Two schedulers approaches are discussed: a static approach where the scheduling is predetermined (exactly the one implemented in PLASMA) and a dynamic approach where decisions are made at runtime.

A. Static scheduling

Developed initially on the IBM Cell processor [16], the static scheduling implemented in PLASMA uses POSIX threads and naive synchronization mechanisms. Figure 9 shows the step-by-step scheduling execution with eight threads on a square tile matrix ($MT = NT = 5$). In this particular figure, the work is distributed by columns of tiles and there are five panel factorization steps, and each of those steps is performed sequentially. It implements a right-looking QR factorization, and the steps of the factorization are pipelined. The cores are mapped on a one dimensional partitioning. The mapping to the tasks is executed before the actual numerical factorization based on a look-ahead of varying depth. The look-ahead strategy greedily maps the cores that might run out of work to the different block column operations. This static approach is well adapted to schedule Algorithm 1 and achieves high performance [4] thanks to an efficient cache reuse [17]. This static scheduling could be

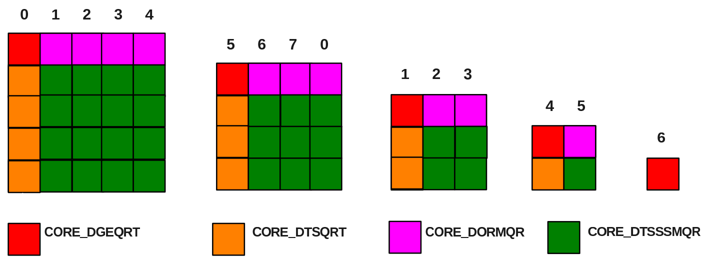

Fig. 9. Work assignment in the static pipeline implementation of the tile QR factorization.

extended to the SP-CAQR algorithm since SP-CAQR performs a PLASMA-like factorization on each domain. However, this would prompt load balancing issues difficult to address with a hand-written code[1]. Another solution consists of using a dynamic scheduler where the tasks are scheduled as soon as their dependencies are satisfied and that prevents cores from stalling.

B. Dynamic scheduling

We decided to present experimental results obtained with a well established and robust dynamic scheduler, SMP Superscalar (SMPSs) [2]. SMPSs is a parallel programming framework developed at the Barcelona Supercomputer Center (Centro Nacional de Supercomputación). SMPSs is a dynamic scheduler implementation that addresses the automatic exploitation of the functional parallelism of a sequential program in multicore and symmetric multiprocessor environments.

SMPSs allows programmers to write sequential applications, and the framework is able to exploit the existing concurrency and use the different processors by means of an automatic parallelization at execution time. As in OpenMP, a programmer is responsible for identifying parallel tasks, which have to be side-effect-free (atomic) functions. However, he is not responsible for exposing the structure of the task graph. The task graph is built automatically, based on the information of task parameters and their directionality.

Based on the annotations in the source code, a source to source compiler generates the necessary code and a runtime library exploits the existing parallelism by building at runtime a task dependency graph. The runtime takes care of scheduling the tasks and handling the associated data.

Regarding its implementation, it follows the same approach as described in [17] in order to get the best performance by drastically improving the scheduling. However, SMPSs is not able to recognize accesses to triangular regions of a tile. For example, if only the lower triangular region is accessed during a particular task, SMPSs will still create a dependency on the whole tile and therefore prevent the scheduling of any subsequent tasks that only use the strict upper triangular region of the same tile. To bypass this bottleneck, we force the scheduler to drop some dependencies by shifting the starting pointer address of the tile back and forth.

C. Execution Traces

Figure 10 illustrates the entire execution flow of Algorithms 1, 3 and 4 on eight cores with MT=16 and NT=2 when tasks are dynamically scheduled based on dependencies defined by the corresponding DAG in Figure 7 (Section IV). Each line in the execution flow shows which tasks are performed by one of the threads involved in the factorization. Figure 10 shows the parallel execution traces. Figure 10.a) outlines the poor parallelism of PLASMA-like Tile QR factorization. Not only is the trace irregular with lots of idle time (white spaces) but also two out of eight cores are actually completely inactive. On the contrary, Figures 10.b) and 10.c), present less idle time and most of the cores are concurrently performing operations. It is also important to mention that the presence of idle time is mainly due to the relative small size of the matrix, i.e., MT=16 and NT=2. The cores run out of work right from the beginning, while such a behavior is more expected toward the end of the factorization when the matrix is large enough. Indeed, Figure 11 shows that all the idle times, which represent the major scalability limit of the fork-join approach, is

[1]One might think to map a constant number of cores per domain, but, after NT panels have been processed, the cores of the first domain would then run out-of-work.

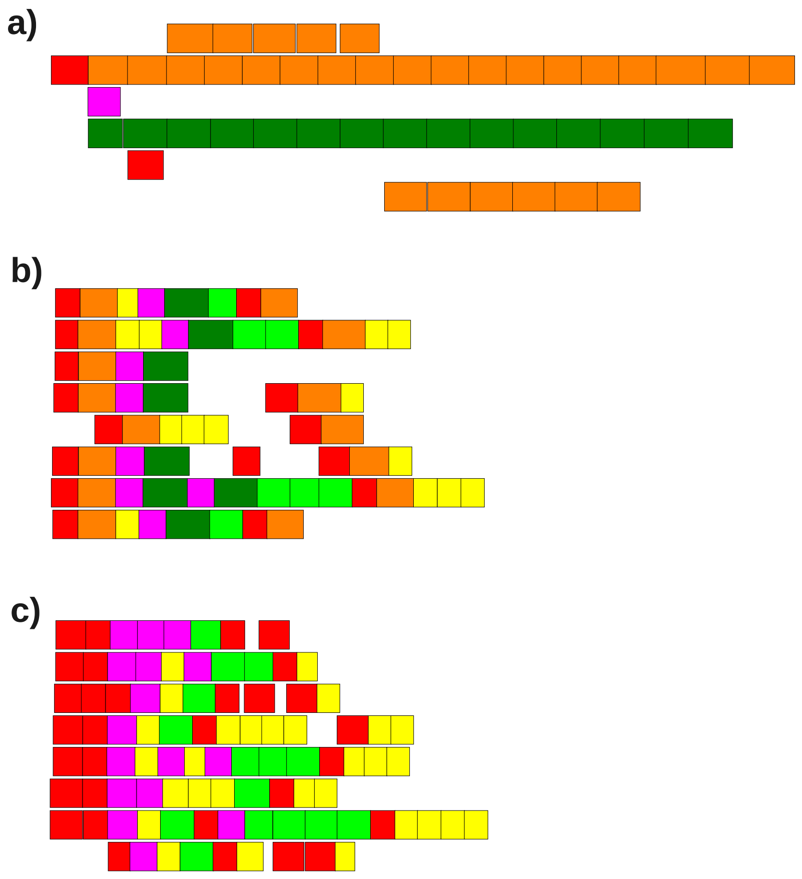

Fig. 10. Parallel execution traces with MT=16 and NT=2 on 8 cores depending on the number of domains. a) One domain: SP-1 (or PLASMA-like Tile QR factorization), b) Eight domains: SP-8, c) Sixteen domains: SP-16 (or FP-CAQR).

removed thanks to the very low synchronization requirements of the graph driven execution.

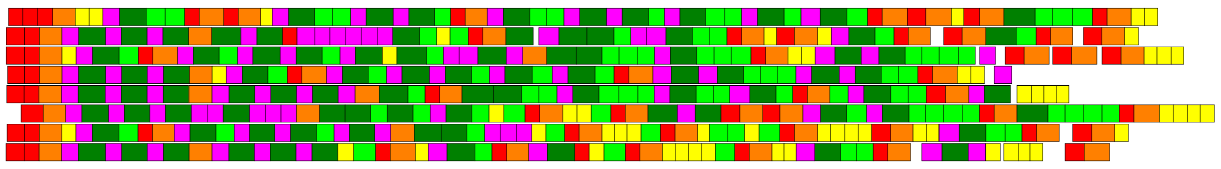

Fig. 11. Parallel execution traces of SP-16 with MT=32 and NT=4 on 8 cores.

In the next section, experimental results of our SP-CAQR algorithm with SMPSs are presented.

VI. Experimental Results

A. Experimental environment

The experiments were conducted on a quad-socket, quad-core machine based on an Intel Xeon EMT64 E7340 processor operating at 2.39 GHz. The theoretical peak is equal to 9.6

Gflop/s/ per core or 153.2 Gflop/s for the whole node, composed of 16 cores. There are two levels of cache. The level-1 cache, local to the core, is divided into 32 kB of instruction cache and 32 kB of data cache. Each quad-core processor being actually composed of two dual-core Core2 architectures, the level-2 cache has 2×4 MB per socket (each dual-core shares 4 MB). The machine is running Linux 2.6.25 and provides Intel Compilers 11.0 together with the MKL 10.1 vendor library [1].

The test matrices were generated by calling DLARNV function from LAPACK. Their values thus follow a pseudo-random uniform distribution. However, since we use the same routine with a consistent seed state, for a given size, all the applications use the same matrix in entry.

The performance of the Tile QR factorization strongly depends on two tunable parameters: the tile size (NB) and the inner blocking sizes (IB) [4]. The tile size trades off parallelization granularity and scheduling flexibility with single core utilization, while the inner block size trades off memory load with extra-flops due to updating factorization techniques [12]. The optimal tile size (NB) and inner blocking size (IB) vary in function of the matrix dimensions (m, n) as discussed in [4]. However, to have a more consistent set of results, we decided to use constant values: NB = 200 and IB = 40. Those values were empirically chosen to maximize the asymptotic performance, the impact of the (NB,IB) on SP-CAQR performance being out-of-the scope of the paper.

We recall that SP-CAQR depends on the number P of domains used, and we note SP-P an instance of SP-CAQR with P domains. If $P = 1$, it corresponds to a PLASMA-like factorization (but SP-1 relies on SMPSs whereas PLASMA implements a static scheduler). On the other side of the spectrum, we recall that $P = MT$ (MT is the number of tiles per row) corresponds to the FP-CAQR algorithm. As discussed in Section V, our SP-CAQR algorithm is scheduled with SMPSs dynamic scheduler.

In this section, we essentially present experiments on TS matrices (where the higher improvements are expected), but we also consider general and square matrices. A comparison against state of the art linear algebra packages (LAPACK, ScaLAPACK, PLASMA) and the vendor library MKL 10.1 concludes the section. All the packages have been linked against the BLAS from Intel MKL.

When we report the Gflop/s rate, we consistently use the number of floating point operations that a standard algorithm would perform. All performance results reported in the paper (SP-CAQR, PLASMA, ScaLAPACK, MKL, LAPACK) are indeed computed using the same algorithmic complexity formula: $2.m.n^2 - 2.n^2/3$ flops. The actual number of floating point operations depends on the algorithm. For instance, SP-CAQR and MKL perform a different number of operations. Furthermore, that number depends on the tile size (NB), the internal blocking size (IB), and the number of domains (P). Indeed, SP-CAQR trades flops for communications.

B. Tall and Skinny matrices

Figure 12 shows the performance obtained on matrices of only two tiles per row, using 16 cores. The plot is under-scaled (the actual theoretical peak performance is 153.2 Gflop/s. The number of tiles per column MT has to be greater than or equal to the number of domains P; for instance, SP-16 can only be executed on matrices of at least $M = 16 * 200 = 3200$ rows, since a tile is itself of order 200. The overall limited performance (at best 12% of the theoretical peak of the machine) shows the difficulty to achieve high performance on

TS matrices. This is mainly due to the Level-2 BLAS operations which dominate the panel factorization kernels.

If the matrix is tall enough, SP-CAQR (if the number of domains is large too) is up to more than 3 times faster than the (PLASMA-like) Tile QR algorithm (SP-1). With such TS matrices, the greater the number of domains, the higher the performance. In particular, For instance SP-32 is optimum on a 6400 by 400 matrix.

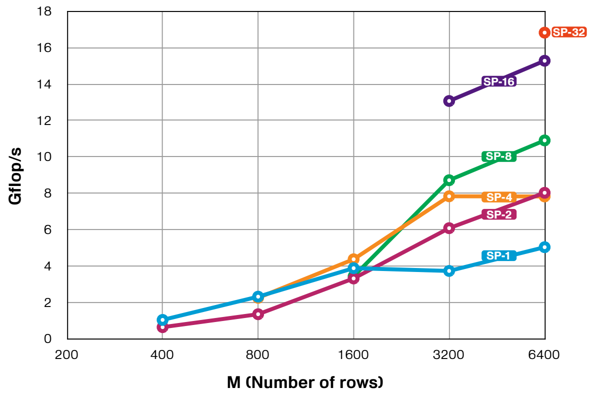

Fig. 12. Performance of 16 core executions on TS matrices with 2 tiles per row ($N = 400$ is fixed).

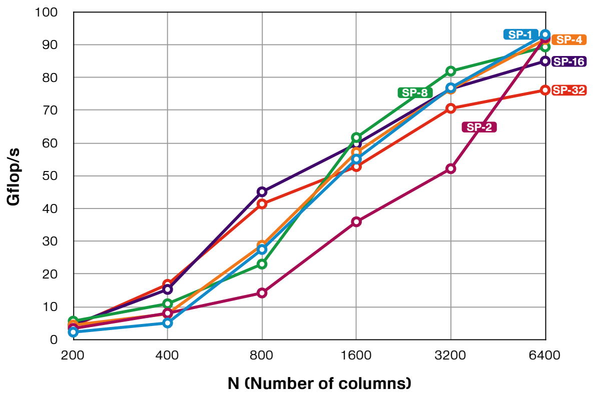

Fig. 13. Performance of 16 core executions on TS matrices with 32 tiles per column ($M = 6400$ is fixed).

Figure 13 shows the performance of matrices with 32 tiles per column on execution using 16 cores. The improvement brought by SP-CAQR is again strong for TS matrices (SP-16 is twice as fast as SP-1 when $N = 800$). However, when the shape of the matrix tends to be square (right part of the graph), PLASMA-like algorithm (SP-1) becomes relatively more and more efficient. It is the fastest execution in the case of the factorization of a square matrix (6400 by 6400). The reason is that, for such large square matrices, the lack of parallelism within the panels is mostly hidden by the other opportunities of parallelism (see Section II-B) and is thus completely balanced by the very good cache usage of PLASMA-like factorizations.

C. Square matrices

Figures 14 and 15 show the performance obtained on square matrices using 8 and 16 cores, respectively. They confirm that the lack of parallelism of PLASMA-like algorithm (SP-1) on small matrices leads to a limited performance and are outperformed by SP-CAQR (SP-P, $P > 1$). On the other hand, PLASMA-like factorization becomes the most efficient approach for matrices of order greater than 3200. Note that the number of tiles per column MT has to be greater than or equal to the number of domains P; for instance, SP-16 can only be executed on matrices of order at least equal to $M = 16 * 200 = 3200$ rows, since a tile is itself of order 200.

D. Comparison with state-of-the-art libraries

In Figure 16, we compare our new approach, SP-CAQR against PLASMA, ScaLAPACK, LAPACK and MKL for a TS matrix of size 51200×3200. SP-CAQR is 27% faster than PLASMA, if the matrix is split in 16 domains (SP-16). Furthermore, for this matrix shape, SP-CAQR is slightly faster when scheduled dynamically (SP-1) than statically (PLASMA)

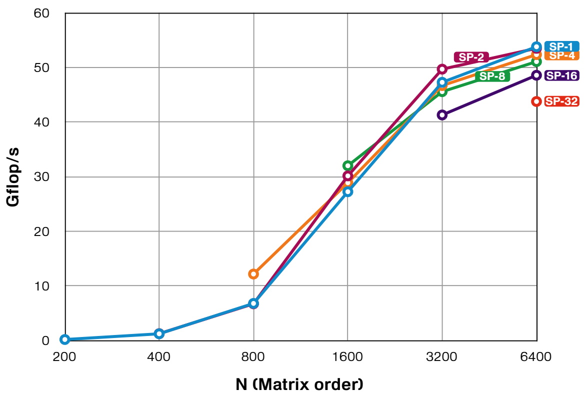

Fig. 14. Performance on square matrices using 8 cores.

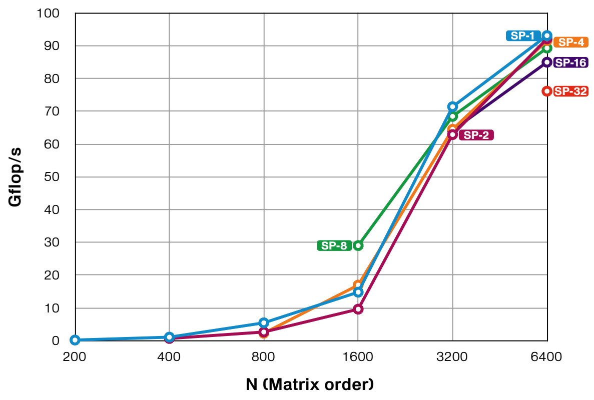

Fig. 15. Performance on square matrices using 16 cores.

with a ratio of 79 Gflop/s against 75 Gflop/s. The performance of SP-CAQR depends on the number of domains. In this case, the most significant performance variation (21%) is obtained between 2 and 4 domains.

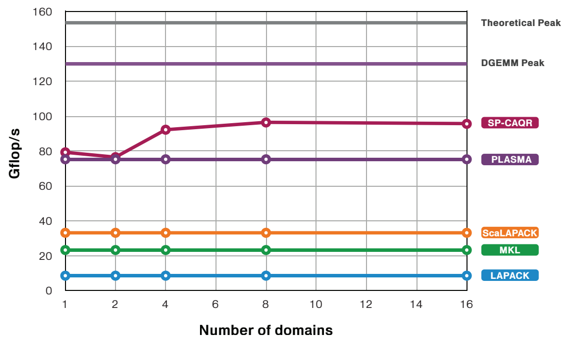

Fig. 16. Performance Comparisons of SP-CAQR depending on the number of domains.

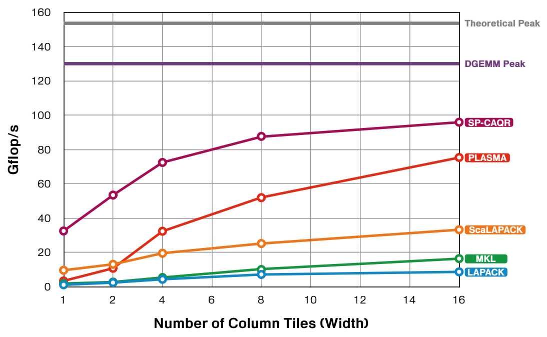

Fig. 17. Scalability of SP-CAQR.

Figure 17 shows the performance on 16 cores of the QR factorization of a matrix where the number of rows is fixed to 51200 and the number of columns varies. For TS matrix of size 51200 by 200, our approach for computing the QR factorization is almost 10 times faster than the Tile QR factorization of PLASMA and around 9 times than MKL (exactly 9.54 and 8.77 as reported in Table III). This result is essentially due to the higher degree of parallelism brought by the parallelization of the panel factorization. It is interesting to notice that the ratio is of order of magnitude of the number of cores, 16, which is clearly an upper bound. LAPACK is around 30 times slower than our approach, while ScaLAPACK is only 3 times slower. By increasing the number of tiles in a column of the matrix, the ratio is less important, however, SP-CAQR is still faster by far compared to state-of-the-art linear algebra packages. PLASMA is performing better and tends to reach the performance of SP-CAQR when the number of tiles in the column are increased. For instance, PLASMA is only 1.27 times slower for matrix size of 51200 by 3200. Regarding the other libraries, the ratio compared to ScaLAPACK is still at 3, while SP-CAQR is more than 4 times and 11 times faster than MKL and LAPACK respectively.

TABLE III
IMPROVEMENT OF SP-CAQR AGAINST OTHER LIBRARIES (PERFORMANCE RATIO).

Matrix sizes	**PLASMA**	**MKL**	**ScaLAPACK**	**LAPACK**
$51200 - 200$	9.54	8.77	3.38	28.63
$51200 - 3200$	1.27	4.10	2.88	11.05

VII. Conclusions and Future Work

By combining two existing algorithms (Tile QR factorization from PLASMA and the CAQR approach), we have proposed a new fully asynchronous and numerically stable QR factorization scheme for shared-memory multicore architectures. We have shown a significant performance improvement (up to almost 10 times faster against previous established linear algebra libraries). We have experimentally assessed the impact of the number of domains on performance, however we have considered only fixed values for the two other tunable parameters (a tile size NB of 200 and inner blocking size IB of 40). We expect to achieve even better performance by tuning those parameters together with the number of domains. In particular, we plan to develop autotuning techniques to achieve an optimum performance. The experiments presented in this paper have been conducted with a well established dynamic scheduler, SMPSs. However, we have also used SP-CAQR with PLASMA's experimental dynamic scheduler [15], making it possible to release SP-CAQR as part of the PLASMA library. We plan to do so when the dynamic scheduler is in a more advanced stage of development.

SP-CAQR also represents a natural building block for extending the PLASMA library to distributed-memory environments. We will indeed benefit from the low amount of communication induced by communication-avoiding algorithms. Furthermore, we plan to investigate the extension of this work to the LU factorization where numerical stability issues are more complex [13].

References

[1] Intel Math Kernel Library (MKL). http://www.intel.com/software/products/mkl/.

[2] SMP Superscalar. http://www.bsc.es/ → Computer Sciences → Programming Models → SMP Superscalar.

[3] E. Agullo, J. Dongarra, B. Hadri, J. Kurzak, J. Langou, J. Langou, and H. Ltaief. PLASMA Users Guide. Technical report, ICL, UTK, 2009.

[4] E. Agullo, B. Hadri, H. Ltaief, and J. Dongarra. Comparative Study of One-Sided Factorizations with Multiple Software Packages on Multi-Core hardware. LAPACK Working Note 217, ICL, UTK, April 2009.

[5] E. Anderson, Z. Bai, C. Bischof, L. Blackford, J. Demmel, J. Dongarra, J. D. Croz, A. Greenbaum, S. Hammarling, A. McKenney, and D. Sorensen. *LAPACK Users' Guide*. SIAM, 1992.

[6] L. S. Blackford, J. Choi, A. Cleary, E. D'Azevedo, J. Demmel, I. Dhillon, J. Dongarra, S. Hammarling, G. Henry, A. Petitet, K. Stanley, D. Walker, and R. Whaley. *ScaLAPACK Users' Guide*. SIAM, 1997.

[7] A. Buttari, J. Langou, J. Kurzak, and J. Dongarra. Parallel tiled QR factorization for multicore architectures. *Concurrency and Computation: Practice and Experience*, 20(13):1573–1590, 2008.

[8] A. Buttari, J. Langou, J. Kurzak, and J. Dongarra. A Class of Parallel Tiled Linear Algebra Algorithms for Multicore Architectures. *Parallel Computing*, 35(1):38–53, 2009.

[9] J. W. Demmel, L. Grigori, M. F. Hoemmen, and J. Langou. Communication-optimal parallel and sequential QR and LU factorizations. LAPACK Working Note 204, UTK, August 2008.

[10] R. W. Freund and M. Malhotra. A Block QMR Algorithm for Non-Hermitian Linear Systems With Multiple Right-Hand Sides. *Linear Algebra and its Applications*, 254(1–3):119–157, 1997.

[11] W. M. Gentleman. Row elimination for solving sparse linear systems and least squares problems. Numer. Anal.,. *Proc. Dundee Conf. 1975, LEct Notes Math*, 506:122–133, 1976.

[12] G. H. Golub and C. F. Van Loan. *Matrix Computation*. John Hopkins Studies in the Mathematical Sciences. Johns Hopkins University Press, Baltimore, Maryland, third edition, 1996.

[13] L. Grigori, J. W. Demmel, and H. Xiang. Communication avoiding Gaussian elimination. In *SC '08: Proceedings of the 2008 ACM/IEEE conference on Supercomputing*, pages 1–12, 2008.

[14] B. Hadri, H. Ltaief, E. Agullo, and J. Dongarra. Tile QR Factorization with Parallel Panel Processing for Multicore Architectures. UT CS Technical Report ut-cs-09-647, UTK, December, 2009, accepted in IPDPS 2010.

[15] J. Kurzak and J. Dongarra. Fully Dynamic Scheduler for Numerical Computing on Multicore Processors. LAPACK Working Note 220, ICL, UTK, June 2009.

[16] J. Kurzak and J. Dongarra. QR factorization for the Cell Broadband Engine. *Sci. Program.*, 17(1-2):31–42, 2009.

[17] J. Kurzak, H. Ltaief, J. Dongarra, and R. M. Badia. Scheduling Linear Algebra Operations on Multicore Processors. LAPACK Working Note 213, ICL, UTK, February 2009.

[18] D. P. O'Leary. The Block Conjugate Gradient Algorithm and Related Methods. *Linear Algebra and Its Applications*, 29:293–322, 1980.

[19] A. Pothen and P. Raghavan. Distributed orthogonal factorization: Givens and Householder algorithms. *SIAM Journal on Scientific and Statistical Computing*, 10:1113–1134, 1989.

[20] R. Schreiber and C. Van Loan. A Storage Efficient WY Representation for Products of Householder Transformations. *SIAM J. Sci. Statist. Comput.*, 10:53–57, 1989.